Brain Stimulation 17 (2024) 112–124

Contents lists available at ScienceDirect

Brain Stimulation

journal homepage: www.journals.elsevier.com/brain-stimulation

Direct subthalamic nucleus stimulation influences speech and voice quality in Parkinson's disease patients

Marine Bobin [a,b], Neil Sulzer [a], Gina Bründler [a], Matthias Staib [a,b], Lukas L. Imbach [b,c,d], Lennart H. Stieglitz [e], Philipp Krauss [e,f], Oliver Bichsel [e], Christian R. Baumann [b,c], Sascha Frühholz [a,b,g,*]

[a] Cognitive and Affective Neuroscience Unit, University of Zürich, 8050 Zürich, Switzerland
[b] Neuroscience Center Zurich, University of Zurich and ETH Zurich, 8057 Zurich, Switzerland
[c] Department of Neurology, University Hospital Zurich, 8091 Zurich, Switzerland
[d] Swiss Epilepsy Center, Klinik Lengg, 8008 Zurich, Switzerland
[e] Department of Neurosurgery, University Hospital Zurich, 8091 Zurich, Switzerland
[f] Department of Neurosurgery, University Hospital Augsburg, 86159 Augsburg, Germany
[g] Department of Psychology, University of Oslo, 0373 Oslo, Norway

ARTICLE INFO

Keywords:
Subthalamic nucleus
Deep brain stimulation
Speech
Voice
Dysarthria
Parkinson's disease

ABSTRACT

Background: DBS of the subthalamic nucleus (STN) considerably ameliorates cardinal motor symptoms in PD. Reported STN-DBS effects on secondary dysarthric (speech) and dysphonic symptoms (voice), as originating from vocal tract motor dysfunctions, are however inconsistent with rather deleterious outcomes based on post-surgical assessments.

Objective: To parametrically and intra-operatively investigate the effects of deep brain stimulation (DBS) on perceptual and acoustic speech and voice quality in Parkinson's disease (PD) patients.

Methods: We performed an assessment of instantaneous intra-operative speech and voice quality changes in PD patients (n = 38) elicited by direct STN stimulations with variations of central stimulation features (depth, laterality, and intensity), separately for each hemisphere.

Results: First, perceptual assessments across several raters revealed that certain speech and voice symptoms could be improved with STN-DBS, but this seems largely restricted to right STN-DBS. Second, computer-based acoustic analyses of speech and voice features revealed that both left and right STN-DBS could improve dysarthric speech symptoms, but only right STN-DBS can considerably improve dysphonic symptoms, with left STN-DBS being restricted to only affect voice intensity features. Third, several subareas according to stimulation depth and laterality could be identified in the motoric STN proper and close to the associative STN with optimal (and partly suboptimal) stimulation outcomes. Fourth, low-to-medium stimulation intensities showed the most optimal and balanced effects compared to high intensities.

Conclusions: STN-DBS can considerably improve both speech and voice quality based on a carefully arranged stimulation regimen along central stimulation features.

1. Introduction

Parkinson's disease (PD) leads to cardinal motor impairments and also affects speech and voice motor behavior. The symptoms include hypokinetic dysarthria [1] and voice dysphonia [2], which are mainly associated with a breathy and harsh voice, reduced voice intensity, monotonic pitch, voice tremor, variable speech rate and rhythm, and an imprecise articulation accuracy [3,4]. One type of PD treatment consists of deep brain stimulation (DBS). DBS in PD typically targets the motor subpart of the subthalamic nucleus (STN-DBS) based on a tripartite subdivision of the STN into a motor, limbic, and associative subpart [5,6]. STN-DBS effectively treats motor dysfunctions in PD [7,8], but there are rather inconsistent results regarding the effects of STN-DBS on the speech and voice quality of PD patients, with studies reporting no effects [9], some partial positive effects [10,11], or profound negative effects [3,12].

* Corresponding author. University of Zurich, Binzmuhlestrasse 14/18, 8050 Zurich, Switzerland.
E-mail address: sascha.fruehholz@uzh.ch (S. Frühholz).

https://doi.org/10.1016/j.brs.2024.01.006
Received 26 July 2023; Received in revised form 21 December 2023; Accepted 16 January 2024
Available online 23 January 2024

While the latter deleterious effects of STN-DBS on speech and voice quality seem a predominant observation, several factors might contribute to the overall mixed results. First, left or right STN stimulation can lead to partly opposing effects, with right STN stimulation having a predominantly positive effect on speech rate and articulation accuracy parameters [13,14], while left STN stimulation seems to further impair speech and voice quality [13,15] and leads to reduced speech intelligibility [16]. Second, STN-DBS can target different spatial locations of STN [17], with reports of speech and voice impairments for more medial or anteromedial [18,19], posterior [11], and posterolateral STN stimulations [15]. The latter posterolateral STN is the typical target for STN-DBS. Dysarthric effects might specifically occur with stimulations at lateral STN boundaries and thus current spreading to adjacent corticobulbar fibers, responsible for controlling muscles in the tongue and larynx [15]. Third, high stimulation intensities usually lead to impaired speech quality, articulation accuracy, and thus intelligibility [18,20], but voice intensity seems unimpaired by high stimulation intensities [20].

Another set of factors concerns the speech and voice assessment procedures. First, clinical perceptual assessment studies predominantly report a general deleterious effect of STN-DBS on speech and voice quality [10,20]. But there are also some reported positive effects in terms of decreased voice tremor [21], sustained phonation abilities [22], and improved voice intensity [3]. Second, computer-based quantifications of acoustic voice features also showed mixed results. Voice jitter and shimmer reflect micro-fluctuations in vocal pitch and intensity, respectively, and both acoustic features were unaffected [15], improved [23], or impaired after STN-DBS [3]. The noisiness of voices, as quantified by the harmonics-to-noise ratio (HNR), seems improved with STN-DBS [23,24] as well as voice intensity [4,20,25]. Third, the post-surgical time gap between STN-DBS implantation and follow-up assessments can considerably influence the assessed degree of impairments, with impairments potentially increasing over time [25].

The effects of STN-DBS on speech and voice quality in PD patients are thus very inconsistent. We here investigated the effects of STN stimulations during the surgery for electrode implantation that allowed us to vary certain stimulation parameters more systematically and to parametrically quantify their effects on speech and voice outcomes. The study had several specific aims. We aimed to obtain a more detailed parametric view of the influence of STN-DBS stimulation parameters (stimulation location, intensity, laterality) on dysarthric and dysphonic symptoms in PD. We accordingly performed several analyses by statistically modeling the relationship between STN stimulation parameters and quantified speech and voice quality features. Specifically, unlike many approaches using post-operative assessments, we performed intra-operative speech and voice assessments in PD patients while varying STN stimulation parameters. It seems that intra-operative speech and voice assessments can be specifically predictive of the influence of STN-DBS on dysarthric and dysphonic symptoms [26]. Post-operative assessments only allow a global assessment of STN-DBS parameters on speech and voice quality parameters, often in a between-group design [14], with little and only time-consuming possibilities for introducing parameter variations and precise information on STN stimulation location. We included both perceptual and computer-based assessments for a full picture of the dysarthric and dysphonic effects in PD. Perceptual assessments follow an approach similar to standard clinical assessments by practitioners. A computer-based assessment allows more detailed, supplemental, and partly more objective speech and voice evaluations. Performing these two different assessments with direct STN stimulation also allows for describing more precisely and comprehensively the functional significance of the STN in the CBTC circuits [27].

2. Materials and methods

2.1. Participants

The study included 38 patients (16 females; mean age 62.55y, SD 8.52, range 34–77; 38 right-handed) who were undergoing bilateral deep brain stimulation (DBS) surgery with the purpose of implanting DBS electrodes in the subthalamic nucleus (STN) for the treatment of idiopathic Parkinson's disease (PD). The surgery took place at the Neurology and Neurosurgery department of the University Hospital of Zurich (Switzerland). All PD patients were undergoing awake surgery for STN-DBS implantation for the treatment of PD. All PD patients were off from any kind of medication and CNS active drugs during the surgery. Patients received only local anesthesia during the surgery and were fully compliant during the course of the surgery and investigation. A full description of the clinical patient characteristics can be found in Table S22, including a description of their non-speech motor scores.

The following inclusion criteria were used to select the patients: (1) diagnosis of PD and no relevant secondary diagnoses (e.g. essential tremor); (2) surgery protocol for bilateral DBS in the STN; (3) German-speaking patients, including native and non-native speakers; (4) availability for pre- and post-scan MR images for the reconstruction of STN stimulation points. From this patient sample, 18 patients were diagnosed with the akinetic-rigid type PD, 7 had tremor-dominant type PD, and 13 had equivalent type PD. See Table S1 for a full description of demographic and clinical PD patient characteristics. All patients gave informed and written consent for the use of their anonymous intra-operative implantation, speech data, neurological data, and brain imaging data for scientific purposes. The study was approved by the cantonal ethics committee of the Swiss Cantone Zurich (KEK-ZH 2017-00400).

2.2. Surgical procedure and STN stimulation

The DBS surgery and intracranial lead implantation were conducted under local anesthesia such that patients were fully awake and oriented during the surgical procedure. A burr hole of 14 mm diameter was applied to the skull of the patient, and a dural incision of 2–3 mm diameter was applied to avoid CSF leakage.

The surgical procedure for the stereotactic implantation of STN-DBS electrodes was then divided into two different steps.

In the first phase, based on pre-operative T1 and T2-weighted MR images and the planned trajectory, up to 5 microtargeting guide cannulas (Cannula STR-021621-00, AlphaOmega Engineering Co. Ltd.) were implanted that allowed the insertion of single microelectrodes for the stimulation of different STN subparts according to stimulation location (central, medial, lateral, anterior, or posterior canal; 2 mm distance of each canal from the central canal) and stimulation depth. The stimulation depth was determined in relation to the target point, which was set to the inferior boundary of the STN. The depth of the target point was set to 0 mm, and any stimulation point superior to the target point was determined in (negative) distance to this target point (−2.33 to −11.44 mm, reported here in the MNI coordinate system after individual brain normalization). The stimulation of STN subparts was done using electrodes (NeuroProbe STR-009080-00, AlphaOmega Engineering Co. Ltd.) inserted in one of the 5 canals and attached to a Neuro Omega system (AlphaOmega Engineering Co. Ltd.) to deliver direct current stimulation in the range of 0–5.5 mA in potential steps of 0.5 mA, with 0 mA meaning no stimulation. During each stimulation condition, we recorded speech samples from patients, and the no stimulation condition (int0 = 0 mA) served as the baseline condition. Most of the patients underwent STN lead implantation in the left and right STN, with the first implantation typically starting in the STN that is opposite to the body side with the strongest PD motor symptoms. Five patients were only stimulated in one hemisphere (4 left, 1 right). Across all patients, the number of stimulation points in the STN, the stimulation

intensities per location point, the order of left and right STN stimulation, and whether only one or both hemispheres have been stimulated differed. Such patient specific features of the stimulation protocol depended on neurological and surgical factors.

The STN supposedly can be divided into three different subnuclei (STN_M motor, STN_A associative, and STN_L limbic) given their differential neural connectivity [28–31] as well as their response profile to STN-DBS [6,32]. STN-DBS for PD patients typically aims to target the motor subpart STN_M, which is the most posterolateral and presumably largest of the three subnuclei of the STN [33]. Since PD patients predominantly suffer from motor impairments that also affect speech motor outcomes, the motor STN_M is the primary DBS target. During this first phase of the STN-DBS surgery, different spatial STN locations especially of STN_M were stimulated (canals of the guide cannula, depth) with different stimulation intensities. For each location and intensity, patients were asked to provide a short speech sample by counting from 1 to 10. In each patient, there were between 1 and 5 left and right locations with STN stimulation (in different canals and with different depths), and each location was stimulated with 1–8 stimulation intensities (0.5 mA or higher). These speech samples were recorded with a microphone (Rode®, Wireless GO, 0.05–20 kHz frequency range, 44.1 kHz sampling rate at 16-bit) that was placed on the patient's thorax approximately 15–20 cm from the mouth.

In the second phase of the surgery, after the optimal stereotactic STN stimulation point was determined and the permanent stimulation location was approved, both the 5-canal guide cannula and the microelectrode were removed, and an intracranial macro-electrode lead (model 3389, Medtronic Inc.) was inserted through the trajectory. After insertion, the macro-electrode was fixated with a titanium Universal Neuro-III micro-plate (Stryker). This macroelectrode was implanted such that typically the second or third of the four contacts of the electrode matched the location of the best stimulation point from the surgical procedure in the first phase. The stereotactic location of this macro-electrode was verified with a post-surgical CT image (post-CT).

2.3. MR and CT image acquisition and analysis

Prior to the STN-DBS surgery, two anatomical images of the patient's brain were acquired. The first image (pre-T1) was a 3D T1-weighted TFE fast gradient echo sequence and had 1-mm isotropic resolution (TR/TE 10.70/6.06 ms, voxel size 1 mm^3, 190 slices, 320 × 320 in-plane matrix). The second image (pre-T2) was a T2-weighted image 3D volume isotropic turbo spin-echo acquisition (VISTA) sequence (TR/TE 2500/256.73 ms, voxel size 1 mm^3, 170 slices, 320 × 320 in-plane matrix). These MR images were acquired on a Philips Ingenia 3T MR scanner. After the surgery and with macro-electrodes implanted, a second CT image was acquired with implanted electrodes visible on this image. The CT image was acquired on a Siemens CT Somatom Definition AS + machine. Non-contrast and venous post-contrast CT head scans were performed on a single-energy Definition AS + scanner with the following scan parameters: tube voltage 120 kVp, quality reference tube current time product 273 mAs per rotation using automated attenuation-based tubecurrent modulation (CARE Dose, Siemens Healthineers), section thickness 0.75 mm, soft-tissue convolution kernel, and filtered back projection reconstruction.

The pre-surgical MR image and the post-surgical CT image were used to reconstruct the stimulation locations in the STN of each patient based on the location of the macro-electrode and the reconstructed micro-electrode stimulation points as inferred from the surgical protocol. All stimulation points for each patient were determined in individual space, transformed to MNI space, and finally combined across patients.

For this procedure, we used the Lead-DBS software (www.lead-dbs.org/) [34] to process and combine the MR and CT images [35]. First, the post-CT image was co-registered to the pre-T1 and pre-T2 images using routines from the Advanced Normalization Tools (ANTs) toolbox, which included multispectral warps with rigid, affine, and non-linear symmetric image normalizations (SyN) algorithms and additional subcortical refinement algorithms [36]. Second, MR and CT images were spatially normalized into MNI space (ICBM 2009b NLIN asymmetric space), applying routines from the ANTs toolbox [36]. In the next step, a brainshift correction method [37] was applied to account for potential brain deformation caused by the skull opening and implanted electrodes, which however should be minimal given the small incision procedure. Subsequently, the four macro-electrode contact points were automatically pre-localized using the Precise and Convenient Electrode Reconstruction (PaCER) method [38]. In some patients, this method failed to reveal a precise electrode contact localization, and therefore the refined TRAC/CORE (trajectory search, contact reconstruction) approach [39] was applied, and the contact location was manually optimized [34]. The reconstructed stimulation locations in the STN are usually quite accurate with routines and algorithms used in the Lead-DBS toolbox (www.lead-dbs.org/) but have a potential error margin of 0.66 mm (SD 0.43) [39]. Finally, we determined the MNI coordinates of all macro-electrode contact points. The MNI coordinates of the contact points helped to determine the exact MNI coordinate of the micro-electrode stimulation sides during the surgery since one of the macro-electrode contacts corresponded to the approved optimal stimulation point from the micro-electrode procedure.

2.4. Stages of data acquisition and dataset description

The datasets for this study were acquired in different stages and settings. First, the speech samples of patients for this study were acquired intra-operatively during a DBS surgery for implanting brain electrodes for STN stimulation. Speech samples were recorded in the neurosurgical unit with a microphone pointed to and located close to the mouth of the patients, which allowed to largely suppress surgical and environmental noise. Second, features of STN stimulations during the surgery were obtained after the surgery from the surgical protocols that were aligned with the timing protocols of the speech recordings. Third, perceptual rating data for the speech samples were obtained after the surgery in standardized settings for experimental auditory experiments with standardized audiological equipment and response devices. All the stages of dataset acquisition and the analysis of the acquired are described in the following sections.

2.5. Speech data acquisition, perpetual ratings, and acoustic feature quantification

Patients were asked to produce simple counting sequences from 1 to 10 in ascending order, and we acquired a total of n = 434 speech samples across the patient sample. Such counting sequences are relatively simple speech tasks that can be easily produced by the patients during surgery and that allow a direct perceptual assessment of speech and voice qualities during the surgery. Counting can be recommended to assess the dysarthric effect in patients with basal ganglia dysfunctions [40] and is easily repeatable in the highly limited settings of the surgery. Furthermore, given that such a counting sequence is also largely phonetically balanced and requires articulatory precision, a computer-based acoustic analysis also allows a detailed quantification of speech and voice parameters.

The speech samples from the counting sequences were recorded with the same microphone for each patient at a 15–20 cm distance from the mouth. Counting from 1 to 10 is a simple speech motor task that allows the intra- and post-operative assessment of speech (dysarthria) and voice quality parameters (dysphonia). All speech samples were checked for major recording and acoustic artifacts. To analyze the speech and voice quality in each counting sequence, we used two different analysis procedures.

First, each counting sequence was perceptually evaluated by human listeners with regard to seven perceptual features. For the perceptual assessment of the voice quality, we used the 5 rating scales that were

taken from the GRBAS inventory [41]. This inventory was demonstrated to have high reliability for ratings [42], and it allows to rate of a voice sample on overall grade of dysphonia, roughness, breathiness, asthenia, and vocal strain (GRBAS). Next to the 5 scales taken from the GRBAS inventory, we asked listeners to rate the speech samples also on the dimension of "articulation accuracy" and of "speech rhythm" as two additional scales, which are more related to speech quality and precision. For all scales, we used a 5-point Likert scale ranging from 1 (does not apply at all) to 5 (applies strongly) for the ratings. After the ratings were acquired, the ratings of articulation accuracy and speech rhythm were inverted compared to the other voice quality scales, such that overall high scores related to a bad voice/speech quality (i.e. more speech and voice impairment) while low scores relate to a good voice/speech quality. The perpetual ratings were provided by an independent sample of 35 raters (29 females, mean age 27y, SD 6.6) with expertise in speech and voice quality assessments (e.g. speech pathologists, speech therapists, phoneticians etc.). Each rater rated a random selection of speech samples out of the total 434 speech samples. Speech samples were randomly assigned to each rater, such that each speech sample received ratings from seven of the raters. The actual number of rated speech samples was $n = 1004$ as part of the broader evaluation purpose for ratings of PD patients during surgery. Out of these 1004 speech samples, only 434 speech samples were included here based on the requirement for baseline recording samples as outlined below.

Second, in order to obtain objective data about the acoustic quality of the speech samples, we analyzed each sample along 62 acoustic features that are related to either speech or voice quality [43,44]. These acoustic features were quantified with established voice/sound analysis tools and procedures, such as the PRAAT toolbox (fon.hum.uva.nl/praat/) and the Voice Analysis Toolbox (github.com/ThanasisTsanas/VoiceAnalysisToolbox). We categorized these 62 features into five different categories, with two categories (speech rate and fluency, imprecise articulation) quantifying features of speech quality (dysarthria), while the other three categories (quality and stability, dysprosody and pitch, intensity parameters) quantifying voice quality (dysphonia). The full set of acoustic features is summarized in Table S2. For each of the five categories, we quantified $n = 8–15$ acoustic features. All features were extracted using established voice analysis tools and procedures that have been shown to reliably quantify PD-related speech and voice features. These features were coded such that higher values would reflect improved speech and voice quality parameters and lower values would reflect speech and voice impairments. All features were z-transformed across the no-stimulation and stimulation conditions before subjecting them to further analyses.

All acoustic features and scores for the rating scales were z-transformed before they were subjected to various statistical analyses. We especially also calculated difference scores for acoustic and perceptual scores by subtracting scores for the baseline condition (0 mA stimulation) from the scores during the STN stimulation (0.5–5 mA). This procedure ensured that speech and voice quality effects during the stimulation period were individually normalized to the no-stimulation condition in each patient. Using the acoustic features and perceptual ratings, we performed several analyses to relate these data with parameters from the stimulation protocol (stimulation depth, intensity).

2.6. Data analysis and major independent variables

Our analysis approaches for the quantified speech and voice quality parameters as dependent variables included several major independent variables according to the STN stimulation protocols, which we want to quickly summarize here before describing the data analysis approaches in more detail (see sections below). The following STN stimulation parameter variations served as major independent variables to explain variations and effects in our dependent variables: (1) STN stimulation intensity level: with "int0" being the no stimulation condition (baseline), and "int1-int4" being stimulation conditions with varying intensity (int1 = 0.5–1 mA, int2 = 1.5–2 mA, int3 = 2.5–3 mA, int4≥3.5 mA); (2) spatial location of STN stimulation: these locations were represented by MNI coordinates along two major spatial directions (z-direction, inferior-to-superior; 45° rotated xy-direction, as a proxy for the medial-to-lateral direction along the extension of the STN); and (3) STN spatial subareas: the definition of these subareas in inferior-to-superior and medial-to-lateral direction resulted from significant effects of stimulating subregions of the STN. Overall, we used these independent variables for many of the analyses that we report in the next sections. We have to note that we did not perform explicit statistical comparisons between the effects of stimulating left and right STN, and any comparisons between left and right stimulation remain descriptive here.

2.7. Analysis of perceptual rating data

Perceptual ratings for the 7 rating scales were first scored for the baseline condition as raw scores. The data were then z-transformed across the no-stimulation (baseline, stim off) and the stimulation conditions (int1-int4, stim on). We then compared the data for all stimulation conditions with the baseline condition separately for the left and the right STN stimulation using a Z-test (right-tailed). FDR correction was applied to account for multiple testing, and the significance threshold for the adjusted p-values was $p < 0.05$.

We then performed a Pearson correlation analysis between the ratings across the 7 rating scales to assess their interdependency. Significant correlations between scales were determined based on the FDR-corrected p-values across all pairwise correlations, with a significance threshold of $p < 1e\text{-}6$.

2.8. Analysis of acoustic speech and voice features

As for the perceptual rating data, the scored acoustic features were z-transformed across the no-stimulation and the stimulation conditions. We first analyzed if the scores for some acoustic features in the no stimulation condition would be significantly below the mean score during stimulation. We used a Z-test (left-tailed) to determine if scores for acoustic features during no stimulation (int0) would be significantly below scores as quantified during the stimulation conditions (int1-int4). FDR correction was applied, and significance was set to $p < 0.05$ for adjusted p-values.

In the next step, we tested if any of the 62 acoustic features would deviate from baseline scores separately for the four intensity levels int1-int4. This analysis was first done by pooling data across the left and right STN stimulation conditions. We tested significance by using a permutation-based randomization approach to obtain significance thresholds. We shuffled the intensity labels for each of the $n = 434$ trials across $n = 2000$ permutations, and this procedure was applied separately for the five feature categories. The original scores were compared against the normal cumulative density function of the permutation distribution, and significance was set to $p < 1e\text{-}4$. The identical analysis was then repeated, but separate analyses were performed for left and right STN stimulation conditions.

Besides this detailed analysis for each single feature for each of the four stimulation intensities, we also performed a summary analysis by calculating the mean scores for the features of each category for each of the four intensity levels. We used a Z-test for the statistical analysis of each category for each intensity level and tested against a normal distribution with mean = 0 and an SD that was estimated across all trials for each condition. FDR correction was applied, and significance was set to $p < 0.05$. This analysis was first performed for all trials pooled across the left and right stimulation points and was then repeated separately for the left and right stimulation conditions.

Using 62 acoustic features for each trial, we finally performed a regression analysis for the purpose of predicting the perceptual ratings for the 7 ratings scales based on the pattern of 62 acoustic features. Specifically, a Lasso regression analysis (normal distribution for the non-

systematic variation, L1 norm) was calculated to predict the perceptual ratings based on the acoustic features. For each perceptual rating scale, the Lasso regression selected only the acoustic features that were able to predict a substantial amount of the variance in the data of the respective perceptual scales and therefore helped to avoid over-fitting. We quantified the R^2_{adj} value to determine the amount of variance explained in the perceptual rating by the variance in the acoustic features.

2.9. Spatial averaging of STN stimulation effects

To obtain spatial subareas of the STN where stimulation effects revealed significant negative (impairments) and positive effects (improvements), we calculated weighted averages for the 7 perceptual rating scales and the 5 major acoustic feature categories along the z-direction (depth) and the rotated xy-direction (laterality, 45° rotation in the xy-plane). Z-transformed and baseline corrected rating and acoustic scores were averaged at every z-level or xy-level, and the mean score at every level was weighted with log(n)+1, with n being the number of trials or observations at each level. With this weighting, the spatial levels with more observations get a higher weight than locations with only a few observations to avoid local effects that are biased by only a few unidirectional observations. The resulting distribution of mean scores was then smoothed with a kernel of n = 4 neighboring elements. This procedure was done for all stimulation trials for the 7 rating scales separately for left and right STN stimulation and was then repeated for each of the 4 stimulation intensities (int1-int4).

We tested for significant effects at the spatial z-levels and xy-levels by using a permutation-based randomization approach to obtain significance thresholds. We shuffled the z-level or the xy-labels for all trials that were the basis of obtaining the mean score distribution across n = 2000 permutations, and this procedure was applied separately for the 7 rating scales and for the 5 feature categories. The original scores were compared against the normal cumulative density function of the permutation distribution, and significance was set to $p < 0.05$.

Based on the identified subareas of significant STN stimulation effects in the z-direction (superior, mid, inferior) and in the xy-direction (lateral, mid, medial), we quantified the mean effects in the spatial subareas for each of the four stimulation intensities (int1-int4). The resulting distribution of mean effects was then fitted with a constant ($y \sim 1$), linear ($y \sim 1 + x$), or quadratic equation ($y \sim 1 + x + x^2$), and these fits were compared in a nested model comparison approach with a significance level of $p < 0.05$. If the quadratic fit was significant and significantly better than the linear fit, we retained the quadratic fit as best describing the data distribution. If only the linear fit was significant and significantly better than the constant fit, we retained the linear fit. If neither of the linear or quadratic fit was significant, the data distribution was classified as non-significantly following a trend.

2.10. Microlesional effects according to the order of left and right STN stimulation

A microlesion effect has often been reported since the introduction of DBS for the treatment of PD [45,46], and it is an additional effect that warrants consideration during quantifying outcome measures of STN-DBS [13]. Insertion of electrodes into brain tissue and DBS lead placement cause microlesions, and such microlesions in dysfunctional brain areas can recreate normal functioning in the targeted brain regions. Concerning the consecutive stimulation of the left and right STN, the assumption of microlesion effects would predict that stimulation on the second hemisphere (microlesion in the first hemisphere plus stimulation effects in the second hemisphere) is superior to stimulation in the first hemisphere (only stimulation effects). To test the possibility that voice and speech improvements are higher in the secondly stimulated STN, we analyzed some of the data by re-ordering them according to a distinction of first and second hemisphere stimulated and performed statistical tests accordingly. From our sample of 38 patients, 25 patients were tested on the left STN first, while 8 patients were tested on the right STN first; 5 patients were only stimulated in one hemisphere and were not included in this analysis.

3. Results

3.1. Intra-operative stimulation was mainly located in the STN motor subpart

To identify the locations of STN stimulation in the patient sample of this study, we first reconstructed the 3D bilateral trajectory of the implanted macro-electrode based on pre- and post-surgical magnetic resonance (MR) and computer-tomographic (CT) images (Fig. 1a). Based on co-registered MR and CT images, we identified the location of the four contact points of the macro-electrode in the individual patient's brain. Given the relative position of the macro-electrode to the approved optimal stimulation during the surgery, we then reconstructed the individual stimulation points based on the known geometry of the surgical guide cannula with five canals and the stereotactic information coded on the surgical protocol (Fig. 1b).

After determining the STN stimulation points in each patient, the stereotactic location of these stimulation points was transformed to the Montreal Neurological Institute (MNI) standard space and pooled across patients. Most of the bilateral stimulation points were located in the motor STN_M covering a broad range from inferior to superior parts of STN_M, while some stimulation points were also located in the neighboring associative STN_A [11] (Fig. 1c). Most of these stimulation points resulted from using the central canal of the guide cannula with a range of the stimulation depth from −2.33 to −11.44 mm from the operative target point (i.e. inferior boundary of each patient's STN) and a range of stimulation intensities in the range 0–5.5 mA in potential steps of 0.5 mA (Fig. 1d). The condition of "0 mA" (no stimulation) served as an individual baseline condition in each patient. There were significantly more stimulations in the left (n = 264) compared to the right STN (n = 170) (Binomial test, $p < 0.001$). This difference in the number of left and right STN stimulations originated from the surgical protocols, which usually imply a first and a denser stimulation of left STN.

3.2. Right STN stimulation ameliorates voice asthenia and articulation accuracy based on perceptual assessments

We first quantified the level of perceptual ratings during the no-stimulation condition after DBS lead implantation (off stimulation, 0 mA stimulation intensity condition), to assess potential speech and voice quality impairments in the patients due to the PD and the lesional effect of the electrode (Fig. 2b, upper panels). This off-stimulation quantification of the speech/voice quality served as a pre-stimulation baseline condition, which largely corresponds to a pre-surgical level of speech/voice performance levels. The overall voice quality rating (GRBAS grade) received a broad distribution of scores with the mean rating (mean 3.39) being slightly above the mid rating point (mid 3.0) towards the positive side of the scale (scale 1–5, 1 = strong impairment, 5 = no impairment at all). This points to some medium impairment in the overall voice quality before STN stimulation. This overall medium voice quality level was specified by medium impairments in the specific features of voice roughness (mean 3.46, SEM 0.14) and asthenia (mean 3.54, SEM 0.16), while voice breathiness (mean 3.85, SEM 0.11) and voice strain (mean 3.95, SEM 0.09) showed higher scores and thus less impairment. In terms of speech quality, speech rhythmicity was rated higher (mean 3.82, SEM 0.08) than articulation accuracy and precision (mean 3.31, SEM 0.14).

In a first general approach, we compared z-transformed scores for the baseline condition with overall effects during stimulation of the left or right STN (Fig. 2b, upper right panel, lower panels). Only for right STN stimulations, we found a significant improvement first as an increase in articulation accuracy (Z-test, n = 38; Z = 2.579, p = 0.017, FDR) and

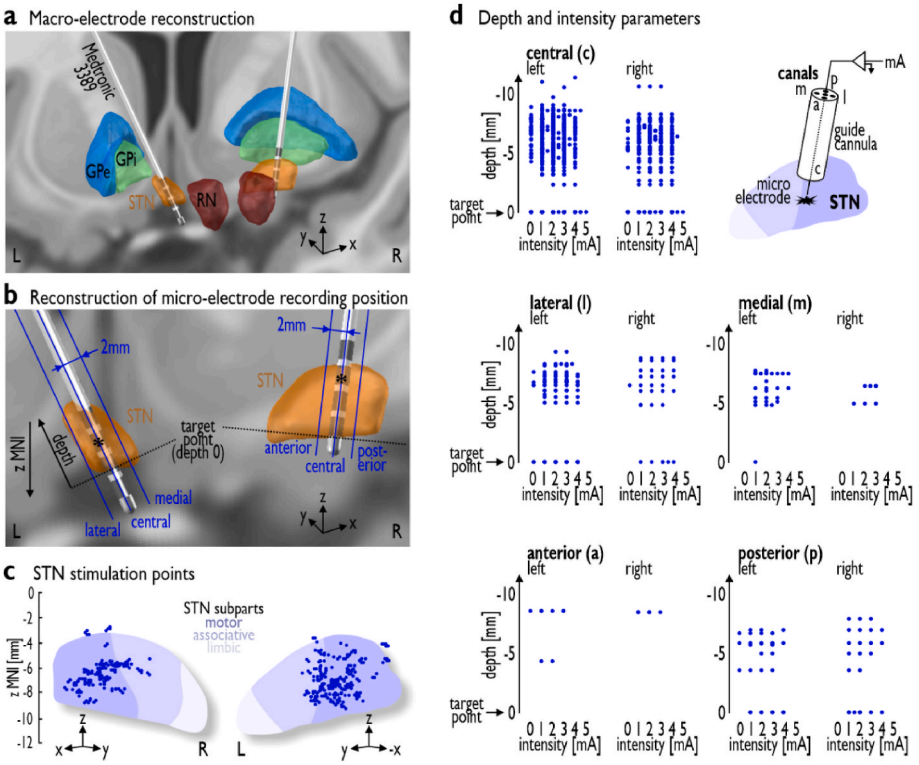

Fig. 1. Intra- and post-operative data about electrode location and stimulation points. (a) Reconstructed trajectories of bilateral macro-electrodes (model 3389 Medtronic) in an exemplary patient targeting the STN (orange) located between the red nucleus (RN, red) and the globus pallidus (GPe/i, blue/green) [61]. (b) The principles of calculating micro-electrode stimulation points (as seen in panel c) based on the macro-electrode trajectory (shown here), the approved point of optimal stimulation (asterisk *), and the relative position of canals of the microtargeting single insertion electrode. The pre-surgically determined target point was the inferior boundary of the STN (depth 0 mm). View in the STN from a 45° angle in the axial plane from the y-axis. (c) All 434 stimulation points (dark blue) in left (n = 264) and right STN (n = 170) across all 38 patients in MNI space; STN subparts as defined by Ewert and colleagues [61]. Stimulation points are plotted with a slight offset in case of spatial overlap; this was done for illustrative purposes here, but not for the analysis of statistical spatial averaging. (d) Summary of stimulation depth across all patients in the left and right STN and across the central, lateral, medial, anterior, and posterior canals. This information is in native space and based on information extracted from the surgical protocols. Stimulation depth is separated according to stimulation intensity. The 0 mA is the off-stimulation condition (baseline); stimulation locations for the baseline condition are reported here but were not used for estimating spatial distribution of effects during the on-stimulation phase; electrode location for the 0 mA condition is also arbitrary because of no STN stimulation. (For interpretation of the references to color in this figure legend, the reader is referred to the Web version of this article.)

second as a decrease in voice asthenia (Z-test, n = 38; Z = 2.621, p = 0.017; FDR correction with adjusted p-values reported) across all stimulation intensity levels. A decrease in vocal asthenia is a sign of improvement (i.e. lower impairment) and is shown in Fig. 2b with a reverse coding. It seems like low and especially medium stimulation intensities (int2-3) are most likely driving these improvements (Z-test, n = 38; Z > 2.873, p < 0.014), while very intense stimulations (int4) did not result in any improvements (Fig. S1). While this is first evidence that STN stimulation can improve specific voice and speech quality features, more detailed effects for the other speech and voice parameters might be revealed when explored for certain stimulation intensity levels (instead of pooling effects for all intensity levels together).

For all further analyses, the z-transformed rating scores were normalized for each patient by subtracting (diff score) the rating score during no stimulation (0 mA, int0) from each rating score during stimulation (e.g. [int1-int0]; with int1 being 0.5–1 mA, int2 being 1.5–2 mA etc.). We first assessed the interdependency between the ratings on each of the voice quality and speech quality scales (Fig. 2c). We found an expected positive correlation between the overall voice quality (overall grade) and the specific voice quality subscales of the GRBAS inventory (Pearson correlation (PC), n = 434; all r's > 0.322, all p's < 10^{-6}, all FDR corrected). Furthermore, all GRBAS subscales were positively intercorrelated (all r's > 0.302), except for vocal strain. Similarly, the two speech scales (articulation accuracy, rhythmicity) were also positively correlated (r = 0.586). Both speech scales were also positively correlated with vocal breathiness (r > 0.384 for both scales) and asthenia (r > 0.381 for both scales).

3.3. *Computer-based acoustic analysis shows differential effects of left and right STN stimulation on voice and speech features*

In a second approach, we used a computer-based analysis of the PD patients' speech samples along central auditory features that are related to speech and voice quality in normal speech but especially to speech/voice deficits in PD patients as described before [43,44,47] (Table S2). The 62 acoustic features belonged to two major categories that reflect speech quality parameters (speech rate and fluency, articulation accuracy) and to three major categories reflecting voice quality parameters (intensity parameters, quality and stability, dysprosody and pitch).

We first analyzed if some of these features would show a significant deviation from the mean of the distribution (mean = 0 based on the z-transformation) already in the baseline condition with no stimulation (Fig. 2d). Most features related to the first category of speech rate and fluency, which quantify features such as the consistency and regularity of speech and speech pause segments, were relatively mean-centered (all Z-tests, n = 38; Z < 0.900, p > 0.184; FDR correction, adjusted p-values), except for some significantly impaired durational voice parameters, such as the total phonation (Z = 1.699, p = 0.046) and speaking time (Z = 1.550, p = 0.049) as well as the degree of voice breaks (Z = 1.786, p = 0.037). Features of the second dysarthria category of articulation

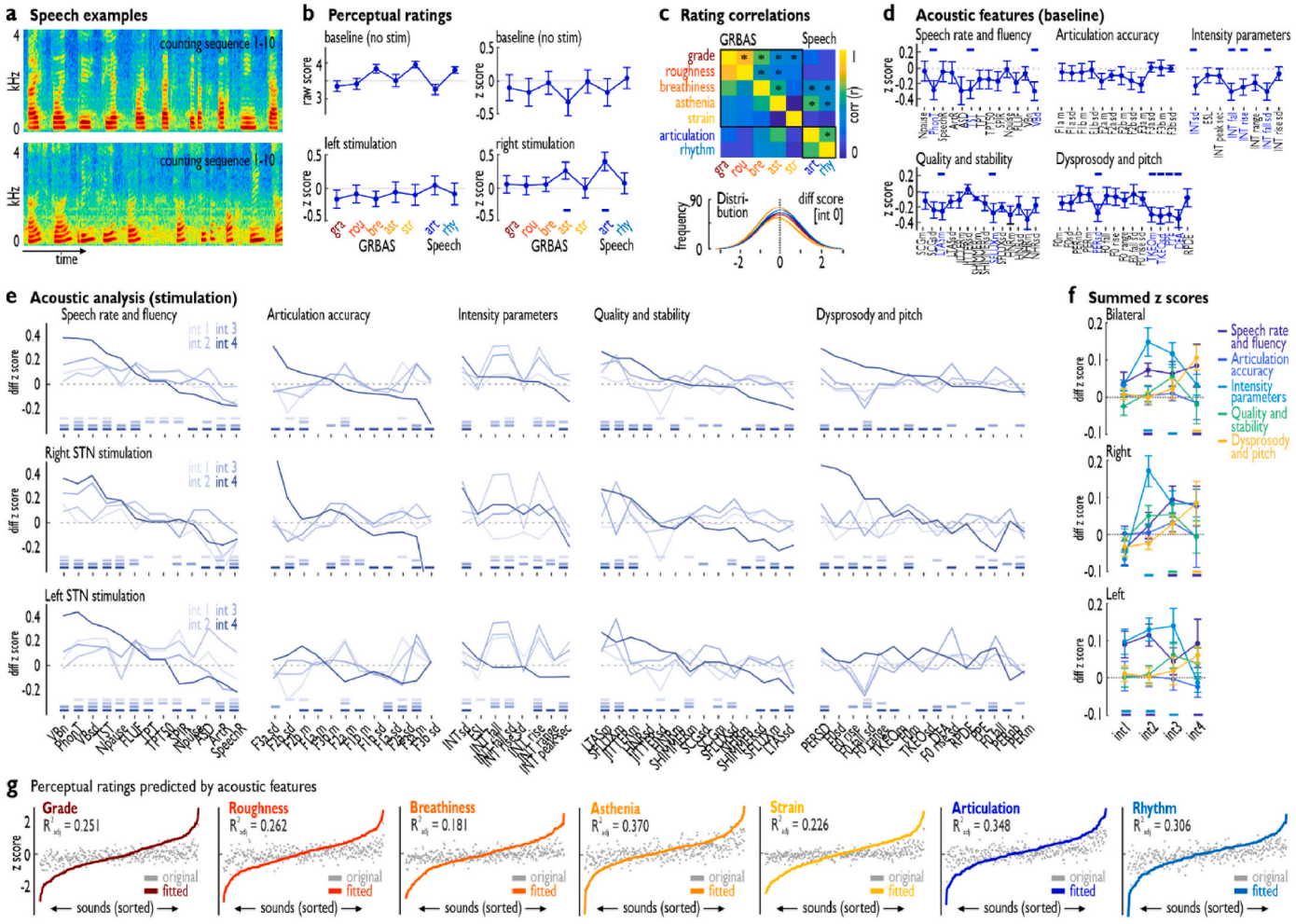

Fig. 2. Acoustic features and perceptual ratings of speech samples. (a) Exemplary spectrograms of two speech samples; upper panel is a speech sample of a rhythmic counting sequence with a clear speech and voice quality; lower panel shows a speech sample with speech and voice quality impairments. (b) Raw (no stim, upper left panel) and z-transformed perceptual rating scores (n = 434, upper right panel) for the five scales of the GRBAS inventory (voice quality) and the two speech quality scales (articulation accuracy, speech rhythm) during the baseline condition. Z-transformed perceptual rating scores for speech samples during left (lower left panel) and right STN stimulation (lower right panel); significant increase in speech and voice quality parameters during stimulation compared to baseline is marked * $p < 0.05$, FDR corrected, (c) perceptual ratings (n = 434) for the five scales of the GRBAS inventory (voice quality) and the two speech quality scales (articulation accuracy, speech rhythm). Upper panel shows the cross-correlation between normalized and z-transformed ratings (*$p < 10^{-6}$, FDR corrected); lower panel shows the distribution of normalized z-transformed rating scores (diff score, baseline value for 0 mA subtracted individually for each patient). (d) 62 acoustic features across five major feature categories belonging to speech quality impairment (dysarthria, i.e. speech rate and fluency, imprecise articulation) and voice quality impairments (dysphonia, i.e. intensity parameters, quality and stability, dysprosody and pitch). Scores are normalized and z-transformed feature scores (z-transformed across all stimulation conditions) during the no-stimulation condition (int0, baseline). Features are pooled and coded such that positive values indicate good quality and negative scores indicate bad speech and voice quality. *$p < 0.05$, FDR corrected. (e) Acoustic speech and voice feature during STN stimulation across the 5 feature categories and separated for four major stimulation intensities (int1 = 0.5–1 mA, int2 = 1.5–2 mA, int3 = 2.5–3 mA, int4≥3.5 mA). Features are sorted for most positive to most negative effects for the int4 condition (dark blue). Small horizontal bars at the bottom of plots indicate significance, $p < 10^{-4}$, permutation statistics. (f) Summed z-scores across all features for each of the 5 feature categories separately for the intensity levels int1-int4. Small horizontal bars at the bottom of plots indicate significance based on Z-tests, $p < 0.05$, FDR corrected. (g) Regression analysis for predicting perceptual ratings for the 7 rating scales based on the pattern of the 62 acoustic features (n = 434). R^2_{adj} values are reported as an indicator of prediction accuracy. The x-axis represents the sounds (voice samples) sorted according to their perceptual rating on the target scale from minimum to maximum rated sounds (based on z-scores). (For interpretation of the references to color in this figure legend, the reader is referred to the Web version of this article.)

accuracy were quantified according to voice formants. Voice formants are spectral maxima resulting from acoustic resonance in the vocal tract and are thus related to the oral cavity motor behavior, and were quantified here especially for voice formants F1–F3. None of these features showed a significant impairment during off-stimulation. The other three categories quantified dysphonic voice features, and we found some voice intensity (i.e. intensity variations, Z = 2.309, p = 0.020; intensity rise, Z = 2.608, p = 0.012; intensity falls, Z = 1.835, p = 0.033; intensity fall variability, Z = 1.820, p = 0.034), voice spectral composition (i.e. long-term average spectrum, Z = 2.478, p = 0.046; spectral flux, Z = 2.792, p = 0.038), and dysprosodic pitch features (i.e. pitch period variation, Z = 2.543, p = 0.033; Teager-Kaiser Energy Operator TKEO mean, Z = 1.674, p = 0.047; TKEO variability, Z = 1.787, p = 0.037; pitch period entropy PPE [48], Z = 1.661, p = 0.048; detrended fluctuation analysis DFA, Z = 2.042, p = 0.021) to be significantly below the mean for the off-stimulation condition.

We then assessed the same set of 62 acoustic features during the STN stimulation condition with varying levels of stimulation intensity (Fig. 2e). Z-transformed and baseline corrected feature scores were tested if they significantly differed from zero, with positive values indicating improvement and negative values indicating impairments (i.e. negative side effects of STN stimulation). For most features and

feature categories, we found that the highest stimulation intensities revealed the strongest speech and voice feature improvements, with the potential exception of intensity parameters (Fig. 2e, upper panels). These speech and voice improvements were more apparent with right STN (Fig. 2e, mid panels) compared to left STN stimulations (Fig, 2e, lower panels). Besides strong improvements with high stimulation intensities for certain voice and speech features, high intensities also led to strong negative effects for some other features, and medium level stimulation intensities seem to have more balanced effects across the set of features. We therefore quantified the overall effects of stimulation intensity in left and right STN by summarizing over the five features categories (Fig. 2f). Summed effects over left and right STN indicated significant effects (Z-tests, $p < 0.05$, FDR corrected) of stimulation intensities int2-int4, with significant improvements for dysarthric features related to speech rate and fluency as well as voice intensity parameters, and improved dysprosody and pitch features, especially at int4 (Fig. 2f, upper panel). This overall pattern of effects was replicated when looking only at right STN stimulation with additional positive effects on quality and stability voice features (Fig. 2f, mid panel), but left STN stimulation revealed a slightly different picture. Left STN stimulation showed only effects on speech but not on voice features, and stronger and more consistent effects were found more for lower to medium stimulation intensities (Fig. 2f, lower panel).

Clinical assessments of speech and voice disorders in PD patients are usually accomplished by a perceptual evaluation of the patient's voice and speech (i.e. clinicians and speech pathologists perceptually listen to a patient's voice and rate the impairment), but this is sometimes accompanied by more objective computer-based assessments, especially of certain voice features [43,44]. To assess how much the computer-based quantification of our 62 speech and voice features can explain perceptual ratings of speech and voice features on the dimensional rating scales, we performed a regression analysis to predict ratings by the acoustic features (Fig. 2g). The acoustic features were found to explain between 18.1 % ($R^2_{adj} = 0.181$) of the variance for voice breathiness and 34.8 % ($R^2_{adj} = 0.348$) for speech articulation accuracy. Thus, acoustic features could explain some part of the perceptual ratings, but not to a high degree, and clinical assessments of speech and voice features seem to require both perceptual and computer-based assessment to provide a fuller picture of dysarthric and dysphonic impairments in PD patients.

3.4. Right rather than left STN stimulation shows overall more positive effects on perceptual speech and voice features

A major feature of STN stimulation concerns stimulation depth (z-direction), which is explored quite extensively during STN-DBS surgery

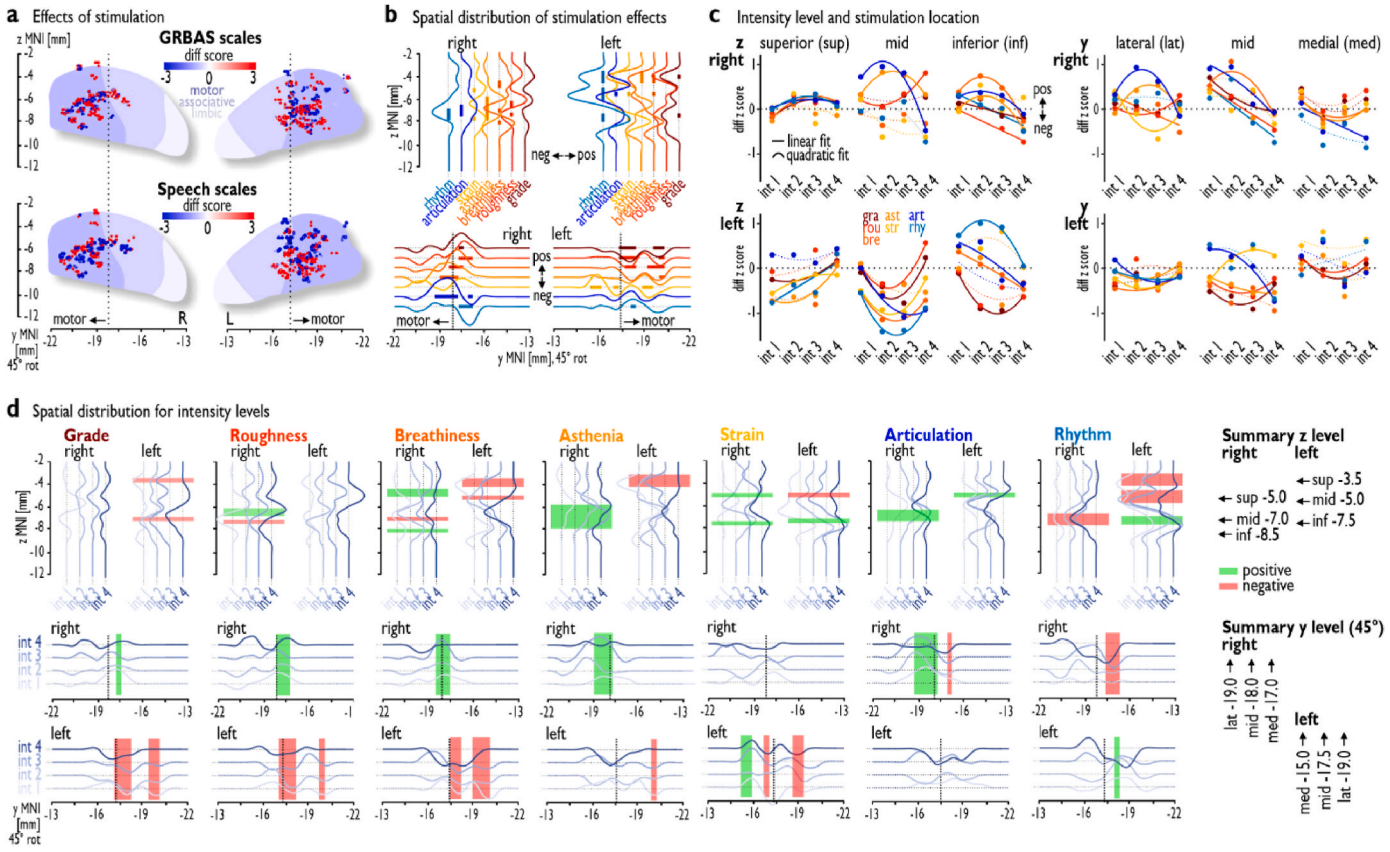

Fig. 3. Effects of stimulation depth and intensity on speech and voice quality perceptual ratings. (a) Summary of DBS effects pooled across all intensity levels in stimulating different STN locations (n = 434). Each dot (red-to-blue scale; difference z-scores) represents a stimulation point; color brightness and dot size indicate the level of the effects (blue = negative effects; red = positive effects). Upper panel shows the stimulation effects as quantified by the five GRBAS scales (voice quality); lower panel shows stimulation effects on the speech scales (speech quality). Dashed vertical lines mark the approximate boundary between the motor and associative subpart of STN. (b) Weighted sum of stimulation effects in superior-inferior direction (i.e. stimulation depth; upper panel) and the medial-to-lateral direction (lower panel; 45° rotation of the x-y axis). Thick bars mark stimulation areas of significant positive or negative effects ($p < 0.05$, permutation statistics). (c) Mean stimulation effects in the superior (sup), mid, and inferior (inf) STN subregions in the z direction as well as in the lateral (lat), mid, and medial (med) subregions in the rotated y direction. Subregions were defined by maximum effects across all scales as shown in b and d (right panel). Data were split for int1 to int4 and were fitted with linear or quadratic equations; bold lines mark significance ($p < 0.05$), dashed lines mark no significance. (d) Same data as in (b) but separated for the different intensity levels (int1 – int4). Green (positive) and red bars (negative) indicate areas of significant effects as marked in (b). (For interpretation of the references to color in this figure legend, the reader is referred to the Web version of this article.)

for optimal stimulation (Fig. 1d). Another spatial feature is stimulation laterality (xy-direction), which shows some but not extensive surgical variation (e.g. by changing micro-electrode insertion in the guide cannula from the central to other canals).

To assess the effects of these spatial features (depth, laterality) together with the feature of stimulation intensity on percental speech and voice ratings, we quantified and summarized these effects along the two major spatial dimensions (Fig. 3).

The z-transformed and baseline-corrected perceptual ratings for the voice (GRBAS) and speech rating scales were first plotted on a representation of the STN in MNI space (Fig. 3a). We then quantified a weighted average (giving more weight to areas with more stimulation points) of these stimulation effects across all stimulation intensities in the z-direction and the xy-direction (Fig. 3b), which allowed identifying subareas of the STN that would lead to speech and voice improvements or impairments with stimulation ($p < 0.05$ permutation statistics). In the left and right STN, we identified three subareas in the z-direction (superior, mid, and inferior in terms of depth) and three subareas in the xy-direction (medial, mid, lateral in terms of laterality) that showed either positive or negative stimulation effects (Fig. 3d). Most of these stimulation sites in the right STN led to positive effects of speech and voice improvements, except for lower and more lateral stimulation sites with negative effects on voice roughness and breathiness as well as speech articulation accuracy and rhythm. Contrarily, most stimulation sites in left STN led to negative speech and voice effects, with the exception of positive effects in inferior STN for voice strain and speech rhythm as well as positive effects in mid-depth STN for speech articulation accuracy.

We additionally quantified the influence of stimulation intensity levels (int1, int2, int3, and int4; see above for the definition of intensity levels) on these spatial effects of STN stimulation (Fig. 3c). We scored the mean effects of stimulation in the three subareas in the z-direction and the three subareas in the xy-direction separately for left and right STN. These scores were then fitted with a linear (i.e. stronger effects with low or high stimulation intensities) or quadratic equation (i.e. strongest effects with medium stimulation intensities) using LME fitting (all $p < 0.05$), and retained the fitting as quadratic if the quadratic fit was significant and significantly better than the linear fit in a nested model comparison, and retained the significant linear fit if no significance was found for the quadratic fit. For the right STN stimulation along the z-direction (depth) (Fig. 3c, left upper panel), most of the fitting resulted in positive quadratic and negative linear fits, indicating that the strongest effects are typically due to low and medium stimulation intensities. For the right STN stimulation in xy-direction (Fig. 3c, right upper panel), the fitting revealed more mixed results, but the strongest effects also followed positive quadratic and negative linear effects, especially for the lateral and mid STN subarea in the laterality direction.

For the left STN stimulation, we again found a partly different pattern. For the left STN stimulation along the z-direction (depth), we mostly found significant negative quadratic fits and a mix of positive and negative linear fits (Fig. 3c, left lower panel). For the superior and mid-level STN subarea, we mainly found negative stimulation effects, with low and medium stimulation levels having the most negative effects (below zero). Only for the inferior STN subarea, there were some positive effects for the low to medium stimulation intensities, specifically for speech rhythm and partly for articulation accuracy [11]. For the left STN stimulation in xy-direction (Fig. 3c, right lower panel), most of the fittings were negative quadratic with mostly about zero and negative stimulation effects. The only exceptions were positive quadratic fits for vocal strain with the strongest effects of high stimulation intensities and for speech articulation accuracy with the strongest effects of lower stimulation intensities. Overall, we found more subareas in the right STN at a mid-depth level and mid-to-lat laterality level, where mostly low-to-medium stimulation intensities led to improvements in speech and voice features. Only some limited left STN subareas led to some positive effects with stimulation in inferior STN at a mid-laterality level.

3.5. Left and right STN stimulation shows positive effects on voice intensity and speech rate acoustic parameters

The previous section reported the effects of stimulating different STN locations, with the effects quantified as perceptual ratings. Our study also included computer-based quantifications of STN stimulation effects on speech and voice quality features. For the latter, we also assessed the effects of stimulating different spatial locations of the STN (Fig. 4) similar to the perceptual ratings. Along the z-direction (depth), we found four different subareas located superior, high mid, low mid, and inferior STN ($p < 0.05$ permutation statistics) (Fig. 4b, upper panel). While we found some subareas with negative effects on dysprosody and pitch features (right inferior), voice intensity features (right high mid), and speech rate and fluency features (left and right inferior, left superior), we also identified two distinct subareas with positive stimulation effects. Voice intensity, as well as speech rate and fluency features, showed improvements with stimulations in both but especially right lower mid STN, with additional positive effects on voice intensity features in superior left and right STN. According to the xy-direction (Fig. 4b, lower panel), these effects were especially pronounced in lateral STN stimulations, with additional positive effects on articulation accuracy with medial right STN stimulations at the border between STN_M and STN_A. High positive effects for speech rate and fluency were achieved for stimulations in bilateral STN_M.

3.6. Small microlesional effects due to the order of stimulated hemispheres

Microlesional effects due to the order of left and right STN stimulation would predict that voice and speech improvements are higher in the second stimulated STN. We therefore analyzed some of the data by re-ordering them according to a distinction of the first and the second hemisphere stimulated (Fig. 5).

According to the perceptual ratings of the speech samples, we did not find a significant effect of improvements (Z-test, $n = 33$; Z's < 1.080, p's > 0.149; FDR corrected) when we compared perceptual ratings during stimulation against ratings when stimulation was off separately for the first and the second hemisphere (Fig. 5a; corresponds to the analysis in Fig. 2b). There were also no significant differences between stimulation effects on the first and second hemisphere (*t*-test, $n = 33$, $t_{31} < 1.527$; p's > 0.860, FDR).

For the acoustic voice and speech features, we performed the same summary analysis for the five categories of features as shown in Fig. 2f, but with data again separated for the first and second hemisphere stimulated (Fig. 5b). First, when determining significant effects separately for the first and second hemisphere, we found that intensity features were improved for int2-int4 (Z-test, $n = 33$; Z's > 2.390, p's < 0.035; FDR corrected), and dysprosody and pitch features were improved for int3-4 (Z-test, $n = 33$; Z's > 2.380, p's < 0.035, FDR) when the first hemisphere was stimulated. A similar pattern of effects was found for stimulation in the second hemisphere for intensity parameters at int2-int3 (Z-test, $n = 33$; Z's > 2.652, p's < 0.016, FDR), and dysprosody and pitch parameters at int3-4 (Z-test, $n = 33$; Z's > 2.730, p's < 0.016, FDR), but with two additional observations. Quality and stability features show enhanced impairments at int1/int4 (Z-test, $n = 33$; Z's < -2.657, p's < 0.040, FDR), whereas speech rate and fluency features showed a significant improvement at int4 (Z-test, $n = 33$; $Z = 4.064$, $p < 0.001$, FDR). While the impairments for the quality and stability features could point to some surgical fatigue effects in patients (i.e. second hemisphere is stimulated after some duration into the surgery), the unique improvements and some increased effects with the stimulation of the second hemisphere could point to some influence of microlesion effects. However, when directly comparing effects for the first and second hemispheres, no significant differences were found (*t*-test, $n = 33$, $t_{31} < 2.120$; p's > 0.528; FDR), pointing to only some minor influence of potential microlesion effects on the outcome data.

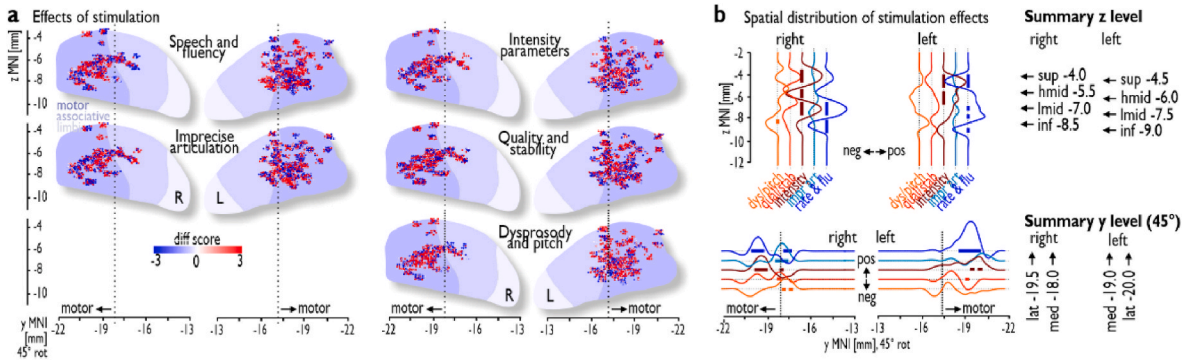

Fig. 4. STN stimulation effects as quantified by acoustic speech and voice features. (a) Summary of DBS effects pooled across all intensity levels (see Fig. 3a). Left panels show the stimulation effects as quantified by speech quality acoustic features; right panels show stimulation effects as quantified by voice quality acoustic features. (b) Weighted sum of stimulation effects in superior-inferior direction (i.e. stimulation depth; upper panel) and the medial-to-lateral direction (lower panel; 45° rotation of the x-y axis). Thick bars mark stimulation areas of significant positive or negative effects ($p < 0.05$, permutation statistics).

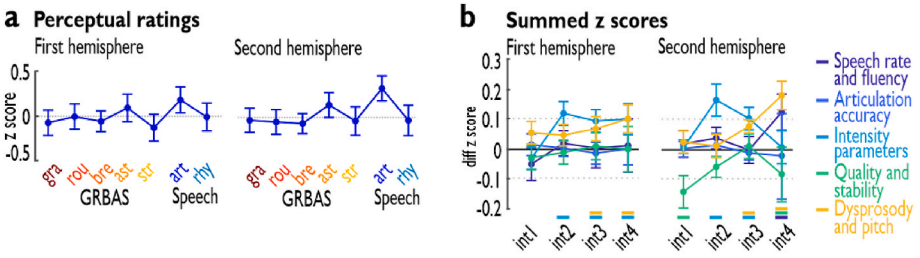

Fig. 5. Microlesion effects of STN stimulation comparing first and second stimulated hemisphere. (a) STN stimulation effects (stimulation on versus stimulation off) on perceptual voice and speech ratings. Shown is the same analysis as in Fig. 2b, but separated between first (left n = 25, right n = 8) and the second hemisphere of STN stimulation. No significant effects were found when comparing stimulation effects against baseline, or when comparing first against second stimulation (all $p > 0.05$, FDR corrected). (b) STN stimulation effects (stimulation on versus stimulation off) on acoustic voice and speech features. Shown is the same analysis as in Fig. 2f, but separated between first (left n = 26, right n = 8) and the second hemisphere of STN stimulation. Small horizontal bars at the bottom of plots indicate significance based on Z-tests, $p < 0.05$, FDR corrected. No significant effects were observed when comparing conditions across the first and second hemisphere (all $p > 0.05$, FDR corrected).

4. Discussion

Our data provide some important findings: (a) there is intraoperative evidence that direct STN stimulation can instantaneously improve speech and voice quality symptoms in PD patients depending on certain stimulation parameters; (b) the assessment of speech and voice quality seems to require both perceptual and computer-based acoustic assessments as both methods show differential effects that are non-redundant; (c) right STN-DBS seems to produce overall more positive effects and seems largely superior to left STN-DBS, while left STN-DBS shows overall strong negative effects (with some exceptions); (d) high stimulation intensities can show the strongest improvements on single and selected perceptual and acoustic features of speech samples, but low and medium stimulation intensities seem to achieve the best effects in terms of balancing symptom improvements and potential side-effects across multiple outcome measures; and (e) the effects of STN-DBS largely depend on the precise location of stimulation, with stronger and more consistent effects in low to mid depth levels (z-level) and rather posterolateral STN subparts (xy-level) that are largely located within the motoric STN_M.

Concerning these latter effects of the spatial STN stimulation site, previous studies were rather coarse in the definition of stimulation site, by defining STN stimulation either as being roughly located inside or outside STN [18,35,49] or being roughly located in the anteromedial, central, or posterolateral STN part [20]. A general assumption of these previous studies was that the best effects were observed with stimulations inside STN and potentially more towards the central and anteromedial STN, roughly representing STN_A and $STN_{L,}$ respectively. Most of our direct STN stimulation points were located within the STN_M as the major target point of STN-DBS, with a minor proportion of stimulation sites located in the neighboring STN_A. We observed negative stimulation effects of this STN_M stimulation on the speech and voice quality of PD patients, which is in line with previous studies [20]. Unlike previous studies, however, we also found strong positive effects of stimulating the posteromedial STN, specifically the STN_M, as well as some positive effects with stimulating neighboring STM_A (mid-level of our laterality factor) close to the STN_M boundary. When quantified with acoustic speech and voice features, STN stimulation overall led to an improved speech quality of PD patients, with right STN stimulation leading to additional positive effects of voice quality features, such as improved quality and stability features as well as dysprosody and pitch features. Previously observed dysarthric worsening with STN macro-electrode stimulations was often attributed to the spread of current to the adjacent corticobulbar fibers, responsible for controlling muscles in the tongue and larynx [15]. This current spread might be less pronounced in intra-operative STN stimulations and opens the potential for observing positive stimulation effects.

A critical factor in STN-DBS concerns the differential effects of left and right STN stimulation [13,14,50–52]. This is important because left STN is assumed to be more tightly linked to speech functions given the predominance of the left brain for speech function in right-handed individuals, while both the left and right brain might regulate certain voice quality features [53]. Left STN stimulation with post-surgical assessments was reported to have strong negative effects, especially on speech quality [19,50]. By estimating the spatial distribution of mean stimulation effects both in the z-direction (depth) and the xy-direction (laterality), we found that left STN stimulations led to overall negative effects when quantified with perceptual ratings. This was evident both

for speech quality and for voice quality assessments. There were only a few exceptions to these overall negative effects. Only very inferior left STN stimulations led to improvements of speech rhythm and voice strain at medium levels of stimulation intensities [54]. Unlike for the left STN stimulation, right STN stimulation led to overall very positive effects on perceptually assessed speech and voice quality parameters. These positive effects were evident across many right STN subareas stimulated, with only a few exceptions of stimulation sites with negative effects and only for the most intense stimulations. Differential effects of left and right STN stimulation could have also been caused by a co-stimulation of the cortico-bulbar tract by DBS-STN, which can cause speech side effects. The corticobulbar tract is located anterior and mostly lateral to STN, but it seems unlikely that co-stimulation of this tract differentially affected our data here. First, at comparable laterality levels we found differential effects on the left and right STN. Second, for the left STN negative effects were found at almost all levels of laterality ranging from medium, mid to lateral levels.

Besides the quantification with perceptual assessment, left and right STN stimulation can also be compared based on the quantified acoustic features. While left STN stimulation showed improved effects on the two major speech quality categories (speech rate and fluency, voice intensity parameters), especially for low to medium stimulation intensities, right STN stimulation led to both improved speech (speech rate and fluency) and voice quality parameters (quality and stability, dysprosody and pitch). And these symptom improvements with right STN stimulation were mainly found for medium to high stimulation intensities. This right-over-left advantage for STN stimulation was also found when we estimated the STN subareas for the effects on the five major acoustic feature categories based on the weighted spatial average. While right STN stimulation led to improvements across all acoustic categories in different xy-subareas, the strongest effects were found for speech rate and fluency parameters and voice intensity parameters in lateral STN in relatively inferior STN stimulation sites. A similar pattern for the latter effects was also found in the left STN. Inferior subareas of the STN are partly located close to the STM_A, and since STM_A is more tightly involved in cognitive functions and cognitive brain circuits [54], more cognitively demanding speech and voice functions might depend on inferior STN.

A final factor that we tested in our study was the influence of stimulation intensity across four major stimulation intensity levels (int1, int2, int3, and int4). Across different analyses, we found that positive and negative effects were found across various levels of stimulation intensities. The most positive and balanced effects across multiple outcome measures were found with medium and rather low stimulation intensities [18,20,55–57], with higher stimulation intensities only positively affecting single voice quality parameters [20], such as dysprosody and pitch parameters (right STN) as well as voice roughness (right STN) and strain (left and right STN). Given that STN-DBS has the major aim to improve the cardinal symptoms of PD, which seems most effective with high stimulation intensities [7,58], these high-intensity stimulations thus seem to have rather negative effects on the speech and voice quality of PD patients [49]. As PD patients experience persisting speech and voice impairments with STN-DBS that even increase with time distance to DBS implantation [26], surgical procedures might therefore want to balance the treatment of general motor symptoms and speech impairments more carefully with optimal STN-DBS stimulation settings [59].

We finally have to mention and discuss a few limitations of the study. First, during speech production and speech sample recordings in our study, patients were lying supine with an anterocollis on the operation table, which is a rather unnatural body position for vocal productions. Ratings of voice and speech quality and potential improvements might have been assessed higher when speech would have been produced in an upright position, but at least all recordings were referenced to an individual baseline recording in the same supine body position. Second, stimulations in the second hemisphere can show additional significant improvements due to the microlesion effects in the first stimulated hemisphere. Some of our data from the acoustic feature analysis pointed in this direction, but the effects were rather small and eventually did not produce significant differences when data from first- and second-hemisphere stimulations were directly compared. This point also seems relevant for the patients with stimulations of only the left or right STN in our sample since microlesional effects are largely absent here. Since major microlesional could not be observed in the patients with left and right STN stimulation, the inclusion of patient with stimulation of only the left or right STN should not introduce a bias here. Third, we found differential effects in left and right STN stimulation. Some of these left-right differences must be taken with some caution since we never directly and statistically compared left versus right STN stimulation effects, which is rather difficult given the variation in the number and localization of stimulation points across patients. This might be precisely accounted for in future studies for direct left-right STN stimulation comparisons.

In conclusion, contrary to many previous reports that pointed to rather negative influences of STN-DBS on voice and speech outcome measures [3,12], this treatment method for PD patients can also have positive effects on their voice and speech quality. About 70–90 % of PD patients experience speech and voice impairments at some stage of the disease [17,60], which also impairs their quality of life. The STN-DBS treatment however often has the priority of mainly improving nonspeech motor symptoms. Nonspeech motor symptoms often seem to be the primary target of surgical procedures with the concurrent aim of avoiding large side effects on speech quality [13]. Our study shows STN-DBS can potentially improve both nonspeech and speech motor behavior at the same time based on a carefully arranged stimulation regimen along central stimulation features. This would altogether improve motor abilities and social communication abilities of PD patients in one treatment setup.

Data availability

The datasets generated within this study cannot be openly shared because they contain patient-sensitive data. The code is available from the lead contact upon reasonable request.

CRediT authorship contribution statement

Marine Bobin: Data curation, Formal analysis, Methodology, Writing – original draft, Writing – review & editing. **Neil Sulzer:** Data curation, Formal analysis, Visualization, Writing – review & editing. **Gina Bründler:** Data curation, Formal analysis, Visualization, Writing – review & editing. **Matthias Staib:** Formal analysis. **Lukas L. Imbach:** Data curation, Formal analysis. **Lennart H. Stieglitz:** Data curation. **Philipp Krauss:** Data curation. **Oliver Bichsel:** Data curation. **Christian R. Baumann:** Data curation. **Sascha Frühholz:** Conceptualization, Data curation, Formal analysis, Funding acquisition, Methodology, Visualization, Writing – original draft, Writing – review & editing.

Declaration of competing interest

The authors declare that they have no known competing financial interests or personal relationships that could have appeared to influence the work reported in this paper.

Acknowledgments

SF supported by the Swiss National Science Foundation (SNSF PP00P1_157409/1 and PP00P1_183711/1 to S.F.). S.F./M.B. also received grant support from the Vontobel Foundation (www.vontobel-stiftung.ch; Zurich, Switzerland).

Appendix A. Supplementary data

Supplementary data to this article can be found online at https://doi.org/10.1016/j.brs.2024.01.006.

References

[1] Polychronis S, Niccolini F, Pagano G, Yousaf T, Politis M. Speech difficulties in early de novo patients with Parkinson's disease. Parkinsonism Relat Disorders 2019;64:256–61. https://doi.org/10.1016/j.parkreldis.2019.04.026.

[2] Brückl M, Ghio A, Viallet F. Measurement of tremor in the voices of speakers with Parkinson's disease. Procedia Comput Sci 2018;128:47–54. https://doi.org/10.1016/j.procs.2018.03.007.

[3] Tanaka Y, Tsuboi T, Watanabe H, Kajita Y, Fujimoto Y, Ohdake R, et al. Voice features of Parkinson's disease patients with subthalamic nucleus deep brain stimulation. J Neurol 2015;262:1173–81. https://doi.org/10.1007/s00415-015-7681-z.

[4] Skodda S, Grönheit W, Schlegel U, Südmeyer M, Schnitzler A, Wojtecki L. Effect of subthalamic stimulation on voice and speech in Parkinson's disease: for the better or worse? Front Neurol 2014. https://doi.org/10.3389/fneur.2013.00218.

[5] Haynes WIA, Haber SN. The organization of prefrontal-subthalamic inputs in primates provides an anatomical substrate for both functional specificity and integration: implications for basal ganglia models and deep brain stimulation. J Neurosci 2013;33:4804–14. https://doi.org/10.1523/JNEUROSCI.4674-12.2013.

[6] Rodriguez-Oroz MC, Rodriguez M, Guridi J, Mewes K, Chockkman V, Vitek J, et al. The subthalamic nucleus in Parkinson's disease: somatotopic organization and physiological characteristics. Brain 2001;124:1777–90. https://doi.org/10.1093/brain/124.9.1777.

[7] Okun MS, Gallo BV, Mandybur G, Jagid J, Foote KD, Revilla FJ, et al. Subthalamic deep brain stimulation with a constant-current device in Parkinson's disease: an open-label randomised controlled trial. Lancet Neurol 2012;11:140–9. https://doi.org/10.1016/S1474-4422(11)70308-8.

[8] Dembek TA, Roediger J, Horn A, Reker P, Oehrn C, Dafsari HS, et al. Probabilistic sweet spots predict motor outcome for deep brain stimulation in Parkinson disease. Ann Neurol 2019;86:527–38. https://doi.org/10.1002/ana.25567.

[9] D'Alatri L, Paludetti G, Contarino MF, Galla S, Marchese MR, Bentivoglio AR. Effects of bilateral subthalamic nucleus stimulation and medication on parkinsonian speech impairment. J Voice 2008;22:365–72. https://doi.org/10.1016/j.jvoice.2006.10.010.

[10] Tsuboi T, Watanabe H, Tanaka Y, Ohdake R, Yoneyama N, Hara K, et al. Distinct phenotypes of speech and voice disorders in Parkinson's disease after subthalamic nucleus deep brain stimulation. J Neurol Neurosurg Psychiatry 2015;86:856–64. https://doi.org/10.1136/jnnp-2014-308043.

[11] Jorge A, Dastolfo-Hromack C, Lipski WJ, Kratter IH, Smith LJ, Gartner-Schmidt JL, et al. Anterior sensorimotor subthalamic nucleus stimulation is associated with improved voice function. Neurosurgery 2020;87:788–95. https://doi.org/10.1093/neuros/nyaa024.

[12] Deuschl G, Schade-Brittinger C, Krack P, Volkmann J, Schäfer H, Bötzel K, et al. A randomized trial of deep-brain stimulation for Parkinson's disease. N Engl J Med 2006;355:896–908. https://doi.org/10.1056/nejmoa060281.

[13] Wang EQ, Metman LV, Bakay RAE, Arzbaecher J, Bernard B, Corcos DM. Hemisphere-specific effects of subthalamic nucleus deep brain stimulation on speaking rate and articulatory accuracy of syllable repetitions in Parkinson's disease. J Med Speech Lang Pathol 2006;14:323–34.

[14] Lin Z, Zhang C, Li D, Sun B. Lateralized effects of deep brain stimulation in Parkinson's disease: evidence and controversies. NPJ Parkinsons Dis 2021;7. https://doi.org/10.1038/s41531-021-00209-3.

[15] Klostermann F, Ehlen F, Vesper J, Nubel K, Gross M, Marzinzik F, et al. Effects of subthalamic deep brain stimulation on dysarthrophonia in Parkinson's disease. J Neurol Neurosurg Psychiatry 2008;79:522–9. https://doi.org/10.1136/jnnp.2007.123323.

[16] Skodda S. Effect of deep brain stimulation on speech performance in Parkinson's disease. Parkinsons Dis 2012. https://doi.org/10.1155/2012/850596.

[17] Zhang F, Wang F, Li W, Wang N, Han C, Fan S, et al. Relationship between electrode position of deep brain stimulation and motor symptoms of Parkinson's disease. BMC Neurol 2021;21. https://doi.org/10.1186/s12883-021-02148-1.

[18] Paek SH, Lee JY, Kim HJ, Kang D, Lim YH, Kim MR, et al. Electrode position and the clinical outcome after bilateral subthalamic nucleus stimulation. J Kor Med Sci 2011;26:1344–55. https://doi.org/10.3346/jkms.2011.26.10.1344.

[19] Tripoliti E, Limousin P, Foltynie T, Candelario J, Aviles-Olmos I, Hariz MI, et al. Predictive factors of speech intelligibility following subthalamic nucleus stimulation in consecutive patients with Parkinson's disease. Mov Disord 2014;29:532–8. https://doi.org/10.1002/mds.25816.

[20] Tripoliti E, Zrinzo L, Martinez-Torres I, Frost E, Pinto S, Foltynie T, et al. Effects of subthalamic stimulation on speech of consecutive patients with Parkinson disease. Neurology 2011;76:80–6. https://doi.org/10.1212/WNL.0b013e318203e7d0.

[21] Hawkshaw MJ, Sataloff RT. Deep brain stimulation for treatment of voice disorders. J Voice 2012;26:769–71. https://doi.org/10.1016/j.jvoice.2012.05.004.

[22] Gentil M, Garcia-Ruiz P, Pollak P, Benabid AL. Effect of bilateral deep-brain stimulation on oral control of patients with Parkinsonism. Eur Neurol 2000;44:147–52. https://doi.org/10.1159/000008224.

[23] Mate MA, Cobeta I, Jiménez-Jiménez FJ, Figueiras R. Digital voice analysis in patients with advanced Parkinson's disease undergoing deep brain stimulation therapy. J Voice 2012;26:496–501. https://doi.org/10.1016/j.jvoice.2011.03.006.

[24] Van Lancker Sidtis D, Rogers T, Godier V, Tagliati M, Sidtis JJ. Voice and fluency changes as a function of speech task and deep brain stimulation. J Speech Lang Hear Res 2010;53:1167–77. https://doi.org/10.1044/1092-4388(2010/09-0154).

[25] Lundgren S, Saeys T, Karlsson F, Olofsson K, Blomstedt P, Linder J, et al. Deep brain stimulation of Caudal Zona Incerta and subthalamic nucleus in patients with Parkinson's disease: effects on voice intensity. Parkinson's Dis 2011;658956:2011. https://doi.org/10.4061/2011/658956.

[26] Kluin KJ, Mossner JM, Costello JT, Chou KL, Patil PG. Motor speech effects in subthalamic deep brain stimulation for Parkinson's disease. J Neurosurg 2022;137:722–8. https://doi.org/10.3171/2021.12.JNS211729.

[27] Foster NN, Barry J, Korobkova L, Garcia L, Gao L, Becerra M, et al. The mouse cortico–basal ganglia–thalamic network. Nature 2021;598:188–94. https://doi.org/10.1038/s41586-021-03993-3.

[28] Krack P, Hariz MI, Baunez C, Guridi J, Obeso JA. Deep brain stimulation: from neurology to psychiatry? Trends Neurosci 2010;33:474–84. https://doi.org/10.1016/j.tins.2010.07.002.

[29] Péron J, Frühholz S, Vérin M, Grandjean D. Subthalamic nucleus: a key structure for emotional component synchronization in humans. Neurosci Biobehav Rev 2013;37:358–73. https://doi.org/10.1016/j.neubiorev.2013.01.001.

[30] Haynes WIA, Haber SN. The organization of prefrontal-subthalamic inputs in primates provides an anatomical substrate for both functional specificity and integration: implications for basal ganglia models and deep brain stimulation. J Neurosci 2013;33:4804–14. https://doi.org/10.1523/JNEUROSCI.4674-12.2013.

[31] Emmi A, Antonini A, Macchi V, Porzionato A, De Caro R. Anatomy and connectivity of the subthalamic nucleus in humans and non-human primates. Front Neuroanat 2020;14. https://doi.org/10.3389/fnana.2020.00013.

[32] Groiss SJ, Wojtecki L, Sudmeyer M, Schnitzler A. Deep brain stimulation in Parkinson-s disease. Ther Adv Neurol Disord 2009;2:379–91. https://doi.org/10.1177/1756285609339382.

[33] Hartmann CJ, Fliegen S, Groiss SJ, Wojtecki L, Schnitzler A. An update on best practice of deep brain stimulation in Parkinson's disease. Ther Adv Neurol Disord 2019;12. https://doi.org/10.1177/1756286419838096.

[34] Horn A, Li N, Dembek TA, Kappel A, Boulay C, Ewert S, et al. Lead-DBS v2: towards a comprehensive pipeline for deep brain stimulation imaging. Neuroimage 2019;184:293–316. https://doi.org/10.1016/j.neuroimage.2018.08.068.

[35] Paek SH, Han JH, Lee J-Y, Kim C, Jeon BS, Kim DG. Electrode position determined by fused images of preoperative and postoperative magnetic resonance imaging and surgical outcome after subthalamic nucleus deep brain stimulation. Neurosurgery 2008;63:925–37. https://doi.org/10.1227/01.NEU.0000334045.43940.FB.

[36] Avants BB, Epstein CL, Grossman M, Gee JC. Symmetric diffeomorphic image registration with cross-correlation: evaluating automated labeling of elderly and neurodegenerative brain. Med Image Anal 2008;12:26–41. https://doi.org/10.1016/j.media.2007.06.004.

[37] Schönecker T, Kupsch A, Kühn AA, Schneider GH, Hoffmann KT. Automated optimization of subcortical cerebral MR imaging-atlas coregistration for improved postoperative electrode localization in deep brain stimulation. Am J Neuroradiol 2009;30:1914–21. https://doi.org/10.3174/ajnr.A1741.

[38] Husch AV, Petersen M, Gemmar P, Goncalves J, Hertel F. PaCER - a fully automated method for electrode trajectory and contact reconstruction in deep brain stimulation. Neuroimage Clin 2018;17:80–9. https://doi.org/10.1016/j.nicl.2017.10.004.

[39] Horn A, Kühn AA. Lead-DBS: a toolbox for deep brain stimulation electrode localizations and visualizations. Neuroimage 2015;107:127–35. https://doi.org/10.1016/j.neuroimage.2014.12.002.

[40] Rusz J, Tykalova T, Ramig LO, Tripoliti E. Guidelines for speech recording and acoustic analyses in dysarthrias of movement disorders. Mov Disord 2021;36:803–14. https://doi.org/10.1002/mds.28465.

[41] Hirano M. Clinical examination of voice: disorders of human communication. Wien: Springer-Verlag; 1981.

[42] Nemr K, Simões-Zenari M, Cordeiro GF, Tsuji D, Ogawa AI, Ubrig MT, et al. GRBAS and cape-V scales: high reliability and consensus when applied at different times. J Voice 2012;26. https://doi.org/10.1016/j.jvoice.2012.03.005. 812.e17–812.e22.

[43] Mucha J, Galaz Z, Mekyska J, Kiska T, Zvoncak V, Smekal Z, et al. Identification of hypokinetic dysarthria using acoustic analysis of poem recitation. In: 2017 40th international conference on telecommunications and signal processing, TSP 2017, vol. 2017- Janua; 2017. p. 739–42. https://doi.org/10.1109/TSP.2017.8076086.

[44] Tsanas A, Little MA, McSharry PE, Ramig LO. Nonlinear speech analysis algorithms mapped to a standard metric achieve clinically useful quantification of average Parkinson's disease symptom severity. J R Soc Interface 2011;8:842–55. https://doi.org/10.1098/rsif.2010.0456.

[45] Tykocki T, Nauman P, Koziara H, Mandat T. Microlesion effect as a predictor of the effectiveness of subthalamic deep brain stimulation for Parkinson's disease. Stereotact Funct Neurosurg 2013;91:12–7. https://doi.org/10.1159/000342161.

[46] Mann JM, Foote KD, Garvan CW, Fernandez HH, Jacobson IVCE, Rodriguez RL, et al. Brain penetration effects of microelectrodes and DBS leads in STN or GPi. J Neurol Neurosurg Psychiatry 2009;80:794–7. https://doi.org/10.1136/jnnp.2008.159558.

[47] Mekyska J, Galaz Z, Mzourek Z, Smekal Z, Rektorova I, Eliasova I, et al. Assessing progress of Parkinson's disease using acoustic analysis of phonation. In: 2015 4th international work conference on bioinspired intelligence (IWOBI). IEEE; 2015. p. 111–8. https://doi.org/10.1109/IWOBI.2015.7160153.

[48] Little MA, McSharry PE, Hunter EJ, Spielman J, Ramig LO. Suitability of dysphonia measurements for telemonitoring of Parkinson's disease. IEEE Trans Biomed Eng 2009;(56):1015–22. https://doi.org/10.1109/TBME.2008.2005954.
[49] Tripoliti E, Zrinzo L, Martinez-Torres I, Tisch S, Frost E, Borrell E, et al. Effects of contact location and voltage amplitude on speech and movement in bilateral subthalamic nucleus deep brain stimulation. Mov Disord 2008;23:2377–83. https://doi.org/10.1002/mds.22296.
[50] Santens P, De Letter M, Van Borsel J, De Reuck J, Caemaert J. Lateralized effects of subthalamic nucleus stimulation on different aspects of speech in Parkinson's disease. Brain Lang 2003;87:253–8. https://doi.org/10.1016/S0093-934X(03)00142-1.
[51] Schulz GM, Hosey LA, Bradberry TJ, Stager SV, Lee LC, Pawha R, et al. Selective left, right and bilateral stimulation of subthalamic nuclei in Parkinson's disease: differential effects on motor, speech and language function. J Parkinsons Dis 2012;2:29–40. https://doi.org/10.3233/JPD-2012-11049.
[52] Wang E, Verhagen Metman L, Bakay R, Arzbaecher J, Bernard B. The effect of unilateral electrostimulation of the subthalamic nucleus on respiratory/phonatory subsystems of speech production in Parkinson's disease – a preliminary report. Clin Linguist Phon 2003;17:283–9. https://doi.org/10.1080/0269920031000080064.
[53] Frühholz S, Schweinberger SR. Nonverbal auditory communication – evidence for integrated neural systems for voice signal production and perception. Prog Neurobiol 2020. https://doi.org/10.1016/j.pneurobio.2020.101948.
[54] Weintraub DB, Zaghloul KA. The role of the subthalamic nucleus in cognition. Rev Neurosci 2013;24:125–38. https://doi.org/10.1515/revneuro-2012-0075.
[55] Krack P, Fraix V, Mendes A, Benabid AL, Pollak P. Postoperative management of subthalamic nucleus stimulation for Parkinson's disease. Mov Disord 2002;17. https://doi.org/10.1002/mds.10163.
[56] Tommasi G, Krack P, Fraix V, Le Bas JF, Chabardes S, Benabid AL, et al. Pyramidal tract side effects induced by deep brain stimulation of the subthalamic nucleus. J Neurol Neurosurg Psychiatry 2008;79:813–9. https://doi.org/10.1136/jnnp.2007.117507.
[57] Törnqvist AL, Schalén L, Rehncrona S. Effects of different electrical parameter settings on the intelligibility of speech in patients with Parkinson's disease treated with subthalamic deep brain stimulation. Mov Disord 2005;20:416–23. https://doi.org/10.1002/mds.20348.
[58] Benabid AL, Chabardes S, Mitrofanis J, Pollak P. Deep brain stimulation of the subthalamic nucleus for the treatment of Parkinson's disease. Lancet Neurol 2009;8:67–81. https://doi.org/10.1016/S1474-4422(08)70291-6.
[59] Boutet A, Madhavan R, Elias GJB, Joel SE, Gramer R, Ranjan M, et al. Predicting optimal deep brain stimulation parameters for Parkinson's disease using functional MRI and machine learning. Nat Commun 2021;12. https://doi.org/10.1038/s41467-021-23311-9.
[60] Levy ES, Moya-Galé G, Chang YHM, Freeman K, Forrest K, Brin MF, et al. The effects of intensive speech treatment on intelligibility in Parkinson's disease: a randomised controlled trial. EClinicalMedicine 2020;24. https://doi.org/10.1016/j.eclinm.2020.100429.
[61] Ewert S, Plettig P, Li N, Chakravarty MM, Collins DL, Herrington TM, et al. Toward defining deep brain stimulation targets in MNI space: a subcortical atlas based on multimodal MRI, histology and structural connectivity. Neuroimage 2018;170:271–82. https://doi.org/10.1016/j.neuroimage.2017.05.015.